21st IMEKO TC4 International Symposium and
19th International Workshop on ADC Modelling and Testing
Understanding the World through Electrical and Electronic Measurement
Budapest, Hungary, September 7-9, 2016

Accurate sine-wave frequency estimation by means of an interpolated DTFT algorithm

Daniel Belega[1], Dario Petri[2], Dominique Dallet[3]

[1]Department of Measurements and Optical Electronics, University Politehnica Timisoara, Bv. V. Parvan, Nr. 2, 300223, Timisoara, Romania, email: daniel.belega@upt.ro
[2]Department of Industrial Engineering, University of Trento, Via Sommarive, 9, 38123, Trento, Italy, email: dario.petri@unitn.it
[3]IMS Laboratory, Bordeaux IPB, University of Bordeaux, CNRS UMR5218,351 Cours de la Libération, Bâtiment A31, 33405, Talence Cedex, France, email: dominique.dallet@ims-bordeaux.fr

Abstract – **An Interpolated Discrete Time Fourier Transform (IpDTFT) algorithm for sine-wave frequency estimation is proposed in this paper. It generalizes the classical interpolated Discrete Fourier Transform (IpDFT) algorithm by interpolating two DTFT spectrum samples located one frequency bin apart. The influence on the estimated frequency of the spectral image component is investigated in the case when the acquired sine-wave samples are weighted by a Maximum Sidelobe Decay (MSD) window. An analytical expression for the estimation error due to the spectral image component is derived. Leveraging on that expression an iterative procedure for the reduction of the effect of spectral image component on the estimated frequency is proposed. The accuracies of the proposed procedure and other state-of-the-art interpolated DFT algorithms are compared by means of both computer simulations and experimental results. It is shown that the proposed procedure can be advantageously adopted when the number of acquired sine-wave cycles is small.**

Keywords **– Discrete Time Fourier Transform (DTFT), Error analysis, Frequency estimation, Windowing**

I. INTRODUCTION

The Interpolated Discrete Fourier Transform (IpDFT) algorithm is often used for sine-wave frequency estimation since it returns accurate results in real-time [1]-[8]. To reduce the detrimental contribution on the estimated frequency of the spectral leakage from narrow band disturbances like harmonics or spurious tones, the analyzed signal is weighted by a suitable window function. Cosine class windows [9] are often employed. In particular, Maximum Sidelobe Decay (MSD) windows allow to obtain very simple IpDFT frequency estimators and exhibit very good spectral leakage suppression capabilities [1]-[8]. Unfortunately, when only few sine-wave cycles are analyzed, IpDFT frequency estimates are heavily affected by the interference from the spectral image component. Multipoint IpDFT methods have been proposed to reduce this detrimental effect [10]-[13]. However, when the number of acquired sine-wave cycles is very small the achieved estimation accuracy is quite low.

In this paper a new Interpolated Discrete Time Fourier Transform (IpDTFT) algorithm is proposed. It generalizes the classical IpDFT approach by interpolating two suitably selected DTFT spectrum samples located one bin apart. The degree of freedom in the selection of the spectrum samples allows to minimize the contribution of the spectral image component on the estimated frequency. An expression for that contribution is derived and - leveraging on that expression - an iterative IpDTFT procedure with maximum Image component interference Rejection capability (called IpDTFT-IR procedure) is proposed. The accuracies of the proposed procedure and other state-of-the-art multipoint IpDFT algorithms are compared through both computer simulations and experimental results.

II. THE PROPOSED IPDTFT ALGORITHM

Let us consider the following discrete-time sine-wave:

$$x(m) = A\sin\left(2\pi\frac{\nu}{M}m + \varphi\right), \quad m = 0, 1, 2, \ldots, M-1 \quad (1)$$

where A, ν, and φ are the amplitude, the number of acquired sine-wave cycles (or normalized frequency expressed in bins), and the initial phase, while M is the number of analyzed samples. The normalized frequency can be expressed as $\nu = l + \delta$, where l represents the closest integer to ν and $-0.5 \le \delta < 0.5$. When coherent sampling occurs δ is null, but usually non-coherent sampling (i.e. $\delta \neq 0$) is encountered in practice.

To reduce spectral leakage, the samples (1) are weighted by a suitable window function $w(\cdot)$ leading to the windowed signal $x_w(m) = x(m)\cdot w(m)$, $m = 0, 1, \ldots, M-1$. The related DTFT can be expressed as [4]:

$$X_w(\lambda)=\frac{A}{2j}\left[W(\lambda-\nu)e^{j\varphi}-W(\lambda+\nu)e^{-j\varphi}\right], \quad (2)$$

where $W(\cdot)$ is the DTFT of the adopted window $w(\cdot)$. It is worth noticing that the second term in (2) is due to the signal image component.

Cosine class windows are often used in spectral analysis. They are defined as:

$$w(m)=\sum_{h=0}^{H-1}(-1)^h a_h \cos\left(2\pi h\frac{m}{M}\right), \ m=0,1,\ldots,M-1 \quad (3)$$

where $H \geq 2$ is the number of window terms, a_h, $h = 0, 1,\ldots, H - 1$ are the window coefficients.

For $|\lambda| << M$ the DTFT of (3) can be expressed as:

$$W(\lambda)\cong\frac{M\sin(\pi\lambda)}{\pi}e^{-j\pi\lambda}\sum_{h=0}^{H-1}(-1)^h a_h\frac{\lambda}{\lambda^2-h^2}. \quad (4)$$

The proposed IpDTFT frequency estimator, as the classical IpDFT algorithm, is based on a two steps procedure [1]:

i) The integer part l of the number of acquired sine-wave cycles is determined through a simple maximum search procedure applied to the DFT samples $|X_w(k)|$, $k = 1, 2,\ldots, M/2 - 1$. If the frequency Signal-to-Noise Ratio (*SNR*) is higher than a known threshold [14], then it is known that l can be exactly determined with very high probability.

ii) The fractional part δ of the number of acquired sine-wave cycles is then estimated by firstly determining the ratio:

$$\alpha_r=\frac{\left|X_w(l+i+(-1)^i r)\right|}{\left|X_w(l-1+i+(-1)^i r)\right|}, \quad (5)$$

where $i = 0$ if $|X_w(l - 1 + r)| \geq |X_w(l + 1 - r)|$, $i = 1$ if $|X_w(l - 1 + r)| < |X_w(l + 1 - r)|$ and $r \in [0, 0.5]$ is the fractional frequency deviation from DFT bins. It is worth noticing that the particular case $r = 0$ corresponds to the classical IpDFT algorithm. Also, when $r = 0.5$ the expression for the ratio α_r does not depend on i.

Using (2) and assuming that the image component provides a negligible contribution to the considered DTFT samples, (5) becomes:

$$\alpha_r\cong\frac{\left|W(-\delta+i+(-1)^i r)\right|}{\left|W(-\delta-1+i+(-1)^i r)\right|}. \quad (6)$$

The IpDTFT fractional frequency estimator $\hat{\delta}_r$ is then obtained by inverting (6) and using the value of α_r returned by (5).

In particular, if the H-term MSD window ($H \geq 2$) is used, (4) becomes [5]:

$$W(\lambda)=\frac{M\sin(\pi\lambda)}{2^{2H-2}\pi\lambda}\frac{(2H-2)!}{\prod_{h=1}^{H-1}\left(h^2-\lambda^2\right)}e^{-j\pi\lambda}. \quad (7)$$

Substituting (7) into (6), after some simple algebra, we obtain:

$$\alpha_r\cong\frac{H-i-(-1)^i r+\delta}{H-1+i+(-1)^i r-\delta}, \quad (8)$$

and the related fractional frequency estimator results:

$$\hat{\delta}_r=\frac{\alpha_r(H+(-1)^i r+i-1)-H+i+(-1)^i r}{\alpha_r+1}. \quad (9)$$

III. THE PROPOSED PROCEDURE

The frequency estimation error due to the spectral interference from the fundamental image component is given by (see Appendix):

$$\Delta\delta_r\cong\left|\Delta\delta_r\right|_{\max}(-1)^H\,\mathrm{sgn}(r+(-1)^i\delta)\cos(2\pi\delta+2\varphi), \quad (10)$$

where:

$$\left|\Delta\delta_r\right|_{\max}\cong\frac{2(l+\delta)(H-r+(-1)^i\delta)}{2l+\delta-(-1)^i H+(-1)^i r}\frac{\left|W(2l+\delta+(-1)^i r)\right|}{\left|W(r-(-1)^i\delta)\right|}. \quad (11)$$

Expression (10) shows that $\Delta\delta_r$ exhibits an almost sinusoidal behaviour with respect to the sine-wave phase φ. The minimum of its amplitude (11) is zero and it is reached when the fractional deviation $r = |\delta|$. Since δ is unknow, that optimal value of r needs to be estimated, for instance, by applying a classical IpDFT algorithm [1]-[8]. Hence, an iterative IpDTFT procedure that maximizes the Image component interference Rejection (IpDTFT-IR procedure) can be implemented. The 10 steps procedure denoted with the acronym IpDTFT-IR(K) - since it is based on K iterations - is described in the following using a pseudo-code:

1. Evaluate the DFT of the windowed signal.
2. Determine the integer part l of the sine-wave frequency by applying a maximum search procedure to the discrete spectrum.
3. Evaluate α_0 by applying (5) on the two largest samples of the discrete spectrum; then determine an initial estimate $\hat{\delta}_0$ for the fractional sine-wave frequency by applying (9) with $\alpha_r = \alpha_0$.
4. $k := 0$ and $r = \left|\hat{\delta}_0\right|$
5. $k := k + 1$
6. Evaluate the two DTFT samples used in (5) and determine

$\alpha_{r,k}$ by applying (5):

$$\alpha_{r,k} = \frac{\left|X_w(l+i+(-1)^i r)\right|}{\left|X_w(l-1+i+(-1)^i r)\right|}$$

7. Determine the fractional frequency estimate $\hat{\delta}_{r,k}$ by applying (9):

$$\hat{\delta}_{r,k} = \frac{\alpha_{r,k}(H+(-1)^i r+i-1)-H+i+(-1)^i r}{\alpha_{r,k}+1}$$

8. Compute $r = \left|\hat{\delta}_{r,k}\right|$
9. Repeat steps 5- 8 *K*-times ($K \geq 1$)
10. Return the fractional frequency estimate obtained at the *K-th* iteration, $\hat{\delta}_{r,K}$.

IV. SIMULATION AND EXPERIMENTAL RESULTS

In this Section the accuracies of the proposed IpDTFT-IR procedure, the classical two-point IpDFT algorithm [2], the improved three-point IpDFT algorithm [13] (called in the following the IpDFT-i algorithm), and the five-point IpDFT algorithm [10] are compared through both computer simulations and experimental results. The two-term MSD (or Hann) window is adopted and $K = 2$ iterations are considered. A number of 1000 runs of $M = 512$ samples each with sine-wave phase selected at random in the range [0, 2π) rad is analyzed. The frequency estimator Mean Square Error (*MSE*) is adopted as accuracy parameter.
Both ideal and noisy sine-waves are considered in the simulation runs.

A. Simulated ideal sine-waves

Fig. 1 shows the MSEs of the considered estimators as a function of ν in the case of ideal sine-waves.

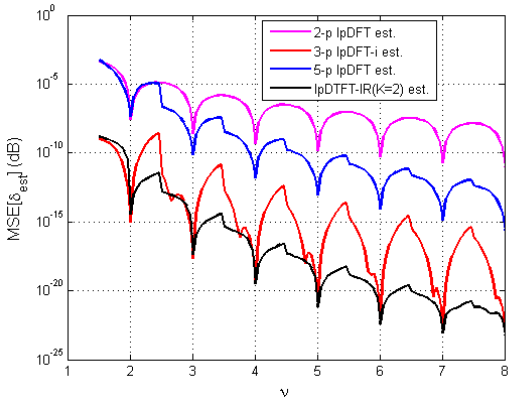

Fig. 1. MSEs of the two-point IpDFT [2], the three-point IpDFT-i [13], the five-point IpDFT [10], and the IpDTFT-IR(2) frequency estimators versus ν in the case of ideal sine-waves. The Hann window is adopted. 1000 runs of M = 512 samples each with sine-wave φ chosen at random.

From Fig. 1 it follows that the proposed estimator outperforms the two-point estimator, the five-point IpDFT estimator, and (in most cases) the IpDFT-i estimator. The poorest performance is achieved by the IpDFT estimator since it is not able to reduce the contribution of the spectral image component.

B. Simulated noisy sine-waves

Fig. 2 shows the MSEs of the considered estimators as a function of ν when analyzing noisy sine-waves with *SNR* = 40 dB. The related Cramér-Rao Lower Bound (CRLB) for unbiased estimators is also shown for comparison purposes.

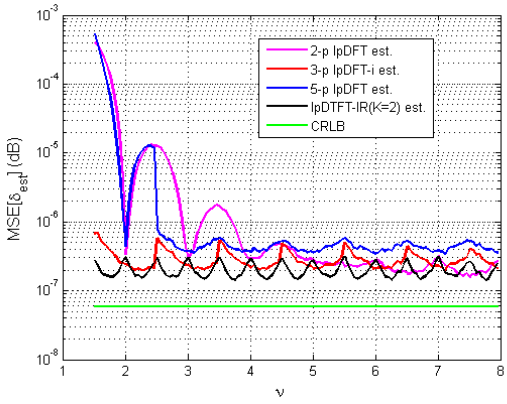

Fig. 2. MSEs of the two-point IpDFT [2], the three-point IpDFT-i [13], the five-point IpDFT [10], and the IpDTFT-IR(2) frequency estimators versus ν. Noisy sine-waves with SNR = 40 dB. The Hann window is adopted. 1000 runs of M = 512 samples each with sine-wave φ chosen at random.

As can be seen, the proposed procedure outperforms the other algorithms, except in quasi-coherent conditions (i.e. when $\delta \cong 0$), and when $\nu > 6$ for $|\delta|$ close to 0.5, where the IpDFT-i algorithm and the two-point IpDFT algorithm, respectively, provide the most accurate results. Fig. 2 shows also that the MSEs of the IpDFT-i estimator and the IpDTFT-IR(2) estimator exhibit the same range of accuracy variations, thus confirming their high spectral image interference rejection capability. Indeed, the differences between the results returned by these two algorithms are quite small, and they are mainly due to the effect of wideband noise, which increases as the number of interpolation points increases [11].
Fig. 3 shows the MSEs of the considered estimators as a function of *SNR* when $\nu = 2.3$ cycles. The *SNR* was varied in the range [0, 100] dB with a step of 5 dB. It is worth observing that the knees of the curves correspond to the *SNR* value above which the effect of the interference from the image component prevails over wideband noise. As can be seen, the proposed procedure provides the highest spectral image component interference rejection among the considered algorithms. The *SNR* value above which the contribution of the spectral image component prevails is equal to about 90 dB, 60 dB, and 20 dB for the proposed procedure, the IpDFT-i algorithm and both two-point and five-point IpDFT algorithms, respectively.

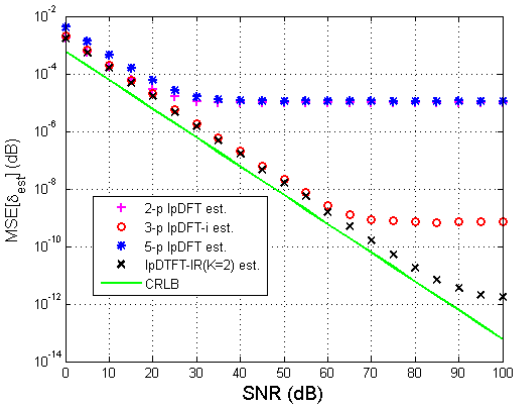

Fig. 3. MSEs of the two-point IpDFT [2], the three-point IpDFT-i [13], the five-point IpDFT [10], and the IpDTFT-IR(2) frequency estimators versus SNR when $\nu = 2.3$ cycles. The Hann window is adopted.1000 runs of $M = 512$ samples each with sine-wave φ chosen at random.

C. Real sine-waves

In the experimental runs, the sine-waves were generated by an Agilent 33220A signal generator and acquired using an NI6023E acquisition board with f_s = 100 kHz sampling frequency and Full Scale Range (*FSR*) = 10 V. The sine-wave amplitude was 2 V and the frequencies varied in the ranges [500, 680] Hz and [1085, 1265] Hz, respectively, with a step of 20 Hz. The related number of acquired sine-wave cycles ν varied in the ranges (2.5, 3.5) and (5.5, 6.5) sine-wave cycles, respectively. The SIgnal-to-Noise And Distortion ratio (*SINAD*) of the acquired sine-waves estimated by means of the four-parameter sine-fitting algorithm [15] was about 60 dB.

Fig. 4 shows the standard deviation of the frequency estimates provided by the considered algorithms as a function of ν. The value of ν was determined as the mean of the estimates returned by the IpDTFT-IR(2) procedure.

As expected from the theoretical and simulation results, Fig. 4 shows that, except in quasi-coherent condition, the proposed procedure outperforms the other considered algorithms. In the quasi-coherent condition the IpDFT-i algorithm slightly outperforms the proposed procedure.

V. CONCLUSIONS

An IpDTFT algorithm for sine-wave frequency estimation that generalizes the classical two-point IpDFT algorithm has been proposed in this paper. An analytical expression for the frequency estimation error due to the spectral image component has been derived. Leveraging on that expression an iterative procedure ensuring a high rejection of the spectral image component effect on the estimated frequency has been proposed in the case when an MSD window is adopted to weight the acquired sine-wave samples. Computer simulations and experimental results show that the proposed procedure outperforms the three-point IpDFT-i algorithm [13] and the multipoint IpDFT algorithms when few cycles of a noisy sine-wave are analyzed.

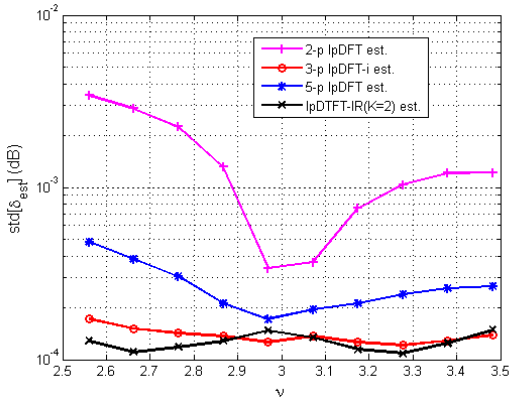

(a)

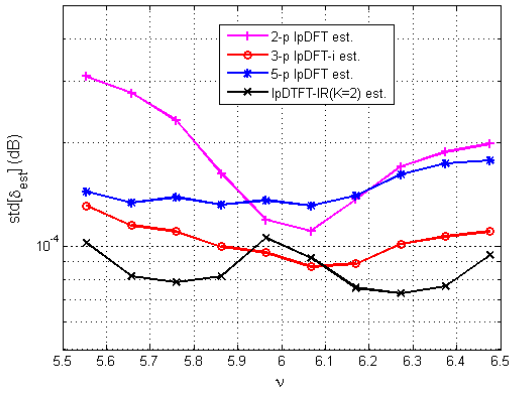

(b)

Fig. 4. Standard deviations of the two-point IpDFT [2], the three-point IpDFT-i [13], the five-point IpDFT [10], and the IpDTFT-IR(2) frequency estimators versus ν. Sine-waves frequencies in the ranges (a) [500, 680] Hz and (b) [1085, 1265] Hz, and SINAD about 60 dB. The Hann window is adopted. 1000 runs of $M = 512$ samples each.

APPENDIX

Derivation of the expression for the error $\Delta\delta$.

Using the identity $|z_1 + z_2|^2 = |z_1|^2 + |z_2|^2 + 2\,\mathrm{Re}\{z_1 z_2^*\}$, where z_1 and z_2 are complex-valued variables, $\mathrm{Re}\{\cdot\}$ denotes the real part of its argument, and $(\cdot)^*$ denotes the conjugation operator, from (2) we have:

$$\begin{aligned}\left|X_w\left(l+k+(-1)^i r\right)\right|^2 = \frac{A^2}{4}\Big[&\left|W\left(k-\delta+(-1)^i r\right)\right|^2 \\ &+\left|W\left(2l+k+\delta+(-1)^i r\right)\right|^2, \\ &-2\,\mathrm{Re}\left\{W\left(k-\delta+(-1)^i r\right)W^*\left(2l+k+\delta+(-1)^i r\right)e^{j2\varphi}\right\}\Big], \\ & k=-1,0,1, \quad r\in[0,\,0.5],\end{aligned} \tag{A.1}$$

Using (7) we obtain:

$$\begin{aligned}&\mathrm{Re}\left\{W\left(k-\delta+(-1)^i r\right)W^*\left(2l+k+\delta+(-1)^i r\right)e^{j2\varphi}\right\}\\&=-(-1)^{H+k}\,\mathrm{sgn}\left(\delta+(-1)^i r\right)\left|W\left(k-\delta+(-1)^i r\right)\right|\\&\times\left|W\left(2l+k+\delta+(-1)^i r\right)\right|\cos(2\pi\delta+2\phi),\end{aligned}\tag{A.2}$$

where sgn(·) is the sign function.
If l is not too small, we have $\left|W\left(k-\delta+(-1)^i r\right)\right| >> \left|W\left(2l+k+\delta+(-1)^i r\right)\right|$. Thus, using the approximation $(1+x)^{1/2}\cong 1+x/2$, when $|x| << 1$, (A.1) and (A.2) provide:

$$\begin{aligned}&\left|X_w\left(l+k+(-1)^i r\right)\right|\cong\frac{A}{2}\Big[\left|W\left(k-\delta+(-1)^i r\right)\right|\\&+(-1)^{H+k}\,\mathrm{sgn}(\delta+(-1)^i r)\left|W\left(2l+k+\delta+(-1)^i r\right)\right|\cos(2\pi\delta+2\phi)\Big]\end{aligned}\tag{A.3}$$

Using (A.3) the ratio α_r returned by (5) becomes:

$$\begin{aligned}\alpha_r&=\frac{\left|X_w(l+i+(-1)^i r)\right|}{\left|X_w(l-1+i+(-1)^i r)\right|}\\&\cong\frac{\left|W(-\delta+i+(-1)^i r)\right|+p\left|W(2l+\delta+i+(-1)^i r)\right|}{\left|W(-\delta-1+i+(-1)^i r)\right|-p\left|W(2l+\delta-1+i+(-1)^i r)\right|},\end{aligned}\tag{A.4}$$

where $p=(-1)^H\,\mathrm{sgn}(r+(-1)^i\delta)\cos(2\pi\delta+2\varphi)$.
Using (7), (A.4) provides:

$$\alpha_r=\frac{H-i-(-1)^i r+\delta}{H-1+i+(-1)^i r-\delta}(1+\varepsilon),\tag{A.5}$$

where

$$\varepsilon=\frac{p\left[\dfrac{\left|W(2l+\delta+i+(-1)^i r)\right|}{\left|W(-\delta+i+(-1)^i r)\right|}+\dfrac{\left|W(2l+\delta-1+i+(-1)^i r)\right|}{\left|W(-\delta-1+i+(-1)^i r)\right|}\right]}{1-p\dfrac{\left|W(2l+\delta-1+i+(-1)^i r)\right|}{\left|W(-\delta-1+i+(-1)^i r)\right|}}.\tag{A.6}$$

From (A.5) it follows that:

$$\delta_r=\frac{\alpha_r(H+(-1)^i r+i-1)-(1+\varepsilon)(H-i-(-1)^i r)}{\alpha_r+\varepsilon+1}.\tag{A.7}$$

Since $\varepsilon << 1$, we obtain:

$$\Delta\delta_r=\hat{\delta}_r-\delta_r\cong\frac{(2H-1)\alpha_r\varepsilon}{(\alpha_r+1)^2}.\tag{A.8}$$

Using (8) it follows that:

$$\frac{(2H-1)\alpha_r}{(\alpha_r+1)^2}\cong\frac{(H-i+\delta-(-1)^i r)(H-1+i-\delta+(-1)^i r)}{2H-1}.\tag{A.9}$$

Noticing that (9) provides:

$$\begin{aligned}&\left|W(-\delta-1+i+(-1)^i r)\right|\\&=\frac{H-\delta-1+i+(-1)^i r}{H-i+\delta-(-1)^i r}\left|W(-\delta+i+(-1)^i r)\right|,\end{aligned}\tag{A.10}$$

and

$$\begin{aligned}&\left|W(2l+\delta-1+i+(-1)^i r)\right|\\&=\frac{2l+\delta-1+i+H+(-1)^i r}{2l+\delta+i-H+(-1)^i r}\left|W(2l+\delta+i+(-1)^i r)\right|.\end{aligned}\tag{A.11}$$

the following expression for ε is derived:

$$\begin{aligned}\varepsilon\cong p&\frac{2(2H-1)(l+\delta)}{(H-1+r-(-1)^i\delta)(2l+\delta+(-1)^i(r-H))}\\&\times\frac{\left|W(2l+\delta+(-1)^i r)\right|}{\left|W(r-(-1)^i\delta)\right|}.\end{aligned}\tag{A.12}$$

Then, by replacing (A.9) and (A.12) in (A.8) it follows that:

$$\Delta\delta_r\cong p\frac{2(l+\delta)(H-r+(-1)^i\delta)}{2l+\delta-(-1)^i H+(-1)^i r}\frac{\left|W(2l+\delta+(-1)^i r)\right|}{\left|W(r-(-1)^i\delta)\right|}.\tag{A.13}$$

From (A.13) the expression (10) it can be easily derived.

REFERENCES

[1] D.C. Rife, G A. Vincent, "Use of the discrete Fourier transform in the measurement of frequencies and levels of tones", Bell Syst. Tech. J., 49, pp. 197-228, 1970.

[2] T. Grandke, Interpolation algorithms for discrete Fourier transforms of weighted signals, IEEE Trans. Instrum. Meas., 32(2), pp. 350 – 355, 1983.
DOI: 10.1109/TIM.1983.4315077

[3] B.G. Quinn, "Estimation of frequency, amplitude, and phase from the DFT of a time series", IEEE Trans. Signal Process., 45(3) pp. 814-817, 1997.
DOI: 10.1109/78.558515

[4] C. Offelli, D. Petri, "The influence of windowing on the accuracy of multifrequency signal parameter estimation", IEEE Trans. Instrum. Meas., 41(2), pp. 256-261, 1992.
DOI: 10.1109/19.137357

[5] D. Belega, D. Dallet, "Multifrequency signal analysis by interpolated DFT method with maximum sidelobe decay windows", Meas., 42(3), pp. 420-426, 2009.
DOI: 10.1016/j.measurement.2008.08.006

[6] C. Offelli, D. Petri, "Weighting effect on the discrete time Fourier transform of noisy signals", IEEE Trans. Instrum. Meas., 40 (6), pp. 972-978, 1991.
DOI: 10.1109/19.119777

[7] P. Carbone, E. Nunzi, D. Petri, "Frequency-domain based Least-squares Estimation of Multifrequency Signal Parameters", IEEE Trans. Instrum. Meas., 49(2), pp.555-558, 2000.
DOI: 10.1109/19.850394

[8] D. Belega, D. Dallet, D. Petri, "Statistical Description of the sine-wave freqeuncy estimator provided by the interpolated DFT method", Measurement, 45(1), pp.109-117, 2012.
DOI: 10.1016/j..measurement.2011.09.010

[9] A.H. Nuttall, "Some windows with very good sidelobe behavior", IEEE Trans. Acoust. Speech Signal Process., 29(1), pp 84–91, 1981.
DOI: 10.1109/TASSP.1981.1163506

[10] D. Agrež, "Dynamic of frequency estimation in the frequency domain", IEEE Trans. Instrum. Meas., 56(6), pp. 2111-2118, 2007.
DOI: 10.1109/TIM.2007.908240

[11] D. Belega, D. Dallet, D. Petri, "Accuracy of sine-wave frequency estimation by multipoint interpolated DFT approach", IEEE Trans. Instrum. Meas., 59(11), pp. 2808-2815, 2010.
DOI: 10.1109/TIM.2010.2060870

[12] C. Candan, "A method for fine resolution frequency estimation from three DFT samples", IEEE Signal Process. Lett., 18(6), pp. 351-354, 2011.
DOI: 10.1109/LSP.2011.2136378

[13] D. Belega, D. Petri, D. Dallet, "Frequency estimation of a sinusoidal signal via a three-point interpolated DFT method with high image component interference rejection capability," Digital Signal Process., 24 (1), pp. 162-169, 2014.
DOI: 10.1016/j.dsp.2013.09.014

[14] E. Aboutanios, "Estimating the parameters of sinusoids and decaying sinusoids in noise", IEEE Instrum. Meas. Mag., 14(2), pp. 8-14, 2011.
DOI: 10.1109/MIM.2011.5735249

[15] *Standard IEEE-1241-2010, "IEEE Standard for Terminology and Test Methods for Analog-to-Digital Converters"* (2011)
DOI: 10.1109/IEEESTD.2011.5692956